Application of enhanced empirical wavelet transform and correlation kurtosis in bearing fault diagnosis

OPEN ACCESS
IOP Publishing
Measurement Science and Technology
Meas. Sci. Technol. **34** (2023) 035023 (8pp)
https://doi.org/10.1088/1361-6501/aca690

Application of enhanced empirical wavelet transform and correlation kurtosis in bearing fault diagnosis

Jijun Xue[1], Hao Xu[1,*], Xiaodong Liu[1], Di Zhang[1] and Yonggang Xu[2]

[1] Mechanical Engineering College, Xi'an Shiyou University, Xi'an, Shaanxi 610065, People's Republic of China
[2] The Key Laboratory of Advanced Manufacturing Technology, Beijing University of Technology, Beijing 100124, People's Republic of China

E-mail: xuhao_9851@163.com

Received 1 July 2022, revised 18 October 2022
Accepted for publication 28 November 2022
Published 21 December 2022

Abstract

The traditional empirical wavelet transform (EWT) based on the Meyer wavelet and scale-space method can decompose a signal into several empirical modes. However, this method is not effective in dealing with strong noise and non-stationary signals, which may lead to modal mixing or even decompose too many invalid components. For this purpose, a method based on the combination of enhanced empirical wavelet transform (EEWT) and correlation kurtosis (CK) is proposed in this paper. Firstly, the EEWT is used to segment the spectrum based on the characteristics of the spectrum fluctuations. It uses the minimum points of the envelope as the boundaries of the segmented spectrum. Secondly, a filter bank is constructed based on these boundaries and a maximum value order statistics filter segments the Fourier spectrum with the adaptive decomposition of the signals. Finally, the envelope spectrum generated by CK is used to screen the bearing fault information, which belongs to the decomposition of a signal into empirical modes, so that the rolling bearing fault can be accurately diagnosed. The method's effectiveness is verified by simulated signal experiments and rolling bearing fault signals. The results show that the performance of the proposed method in this paper is better than that of the traditional EWT. Therefore, the method can be applied to the field of bearing faults or other mechanical fault diagnosis directions.

Keywords: empirical wavelet transform, correlation kurtosis, order statistics filter, non-stationary signal, fault diagnosis

(Some figures may appear in colour only in the online journal)

1. Introduction

Rotating machinery, which has been developing rapidly in the research of rolling bearing fault diagnosis, is widely used in industrial systems, such as fans, turbines, lathes, propellers, engines, centrifuges and so on. However, rolling bearings perform an indispensable role in rotating machinery [1].

According to research, the rolling bearing under constant speed has rhythm when it fails. When the inner ring or outer ring of the rolling bearing is damaged, the balls will hit the damaged position one by one. Since the bearing is a standard part in mechanical equipment, there are standards and requirements for the number and size of balls inside the bearing of the same type, so the period or frequency of balls hit the damaged location can be calculated. When analyzing

* Author to whom any correspondence should be addressed.

the vibration acceleration signal during bearing operation, it is found that the signal will contain many pulses and these pulses will show a certain periodicity. Signal processing methods for rotating machinery have been vigorously developed [2]. Huang *et al* [3] proposed an empirical mode decomposition (EMD) method that relies on signal extreme points which can decompose a signal into several intrinsic mode components. Feng and Chu [4] combined EMD and Hilbert transform demodulation to realize the frequency demodulation analysis of the vibration signal of the planetary gearbox. Lei *et al* [5, 6] combined EMD, Hilbert transform and wavelet packet transform to extract additional fault feature information in order to identify different damage modes of gears. However, the preconditions of EMD execution are difficult to be satisfied by noise signals and non-stationary signals, which leads to a series of data-driven modal decomposition methods, such as local mean value decomposition, which are prone to endpoint effect and modal aliasing. Rehman *et al* [7–9] proposed multivariate EMD and added white noise to the bearing vibration signal. This noise-assisted multivariate EMD method can effectively suppress modal aliasing. Li *et al* [10] constructed the envelope mean value function and envelope estimation function through the Hermite interpolation method to calculate the mean value of adjacent extreme points, which can restrain modal aliasing to a certain extent. The analytical modal decomposition method proposed by Chen and Wang [11] can divide a signal into high-frequency and low-frequency components according to the selected frequency in Wang *et al* [12]. The method proposed by Zhang *et al* [13] can avoid overlapping high-frequency components and low-frequency components in the frequency domain, but it cannot guarantee that all components in a signal are completely separated. Wei *et al* [14] proposed a new method termed optimal variational mode decomposition to extract rolling bearing fault features, which is more effective and demonstrates superiority over empirical mode decomposition, local mean decomposition and wavelet packet decomposition.

A method of effective feature extraction plays an important part in realizing fault diagnosis of rolling bearings. Since rolling bearings generally operate in an environment with a lot of noise and redundant components that can easily lead to band breakage, empirical wavelet transform (EWT) is used to extract features. Gilles [15] proposed EWT based on the Meyer wavelet can split a signal from the frequency spectrum and the midpoint or the minimum value of the adjacent maximum value is used as the boundary to construct the filter bank. EWT was utilized by Cao *et al* [16] to diagnose faults in railway bearings with non-stationary signals. Zhu and Feng [17] improved EWT by constructing an orthogonal wavelet filter bank and it can better overcome the interference of noise components on sub-band division. Duan and Zhang [18] improved the EWT by pre-setting the number of single components and applying it to the fault diagnosis of planetary gearboxes. Moreover, EWT is also used in bearing fault diagnoses. Cao *et al* [16] used EWT in wheel bearing fault detection and verified a good performance of EWT in the detection of outer race fault, roller fault, and the compound fault of outer race and roller. Chen *et al* [19] proposed an EWT based compound fault diagnosis is method for generator bearing of wind turbine, which showed its effectiveness in weak fault and compound fault diagnosis method. Jiang *et al* [20] uses EWT to separate the inner ring fault portion of the bearing signal from the outer ring fault portion and uses the Duffing oscillator to identify the fault information. Early fault detection of rolling bearings is a challenging task since weak fault features are disturbed by heavy background noise, therefore Yao *et al* [21, 22] proposed a periodicity-enhanced sparse representation method to address this issue. Futhermore, He *et al* [23] proposed maximum correlation kurtosis deconvolution as an effective means to identify periodic pulses of faulty signals, because correlation kurtosis (CK) can measure the index of periodic transient pulse in the vibration signal and generate envelope spectrum. With this envelope spectrum, the bearing fault information can be filtered out. The fault information belongs to a signal decomposition into empirical modes.

Although the method in the above reference implements the application of EWT, it does not reduce the number of invalid components of the original method segmentation, nor does it consider the relationship between the fluctuation characteristics of spectrum and signal. Aiming at the characteristics of bearing faults, this paper proposes a new method that combines enhanced empirical wavelet transform (EEWT) with CK. On the one hand, the fault information in a signal is separated from a noise. On the other hand, the components containing the fault information are screened. Finally, the research results show that the new method can be applied to bearing fault diagnosis.

The rest of the paper is organized as follows. Section 2 briefly reviews the theoretical background the EWT and the CK. Subsequently, section 3 establishes the proposed method in detail and shows the flow chart. In section 4, the proposed method is used to analyze the simulated signal and the CK is used to generate the envelope spectrum to filter the bearing fault information from the decomposition of a signal into empirical modes. In section 5, experimental vibration signals are used to verify the effectiveness of the proposed method. Finally, conclusions are given in section 6.

2. Fundamental theories

2.1. Steps of empirical wavelet transform

The implementation steps of EWT are as follows [15].

Step1: The frequency domain of the Fourier transformed signal $f(t)$ is normalized to $[0,\pi]$, which is divided into N frequency bands of unequal bandwidth to obtain its corresponding spectrum $f(\omega)$.

Step2: The local maximum point of $f(\omega)$ is found in the spectrum of the signal and arranged in descending order. The frequency domain of the signal is segmented according to the maximum value points. Setting that ω is the boundary between each frequency band, the left boundary is $\omega_0 = 0$, the right boundary $\omega_N = 0$, and the remaining boundaries can be expressed as ω_1, ω_2,…, ω_N. Therefore, each frequency band can be recorded as $\Lambda_n = [\omega_{n-1}, \omega_n]$, $n = 1,2,\ldots N$. It is obvious that $\cup_{n=1}^{N} \Lambda_n = [0,\pi]$. At this time, a transition segment with a

width of $T_n = 2\tau_n$ is defined with each boundary as the center to construct the window base.

Step3: According to the definition of empirical wavelet, a suitable band-pass filter is constructed for each frequency band. Based on the Meyer wavelet, a set of trigonometric functions that are orthogonal to each other is designed at the two boundaries of a frequency band, and a constant is designed at the frequency band. The empirical scale function $\phi_n(\omega)$ and empirical wavelet function $\psi_n(\omega)$ are constructed according to the frequency segmentation in step 2 as follows

$$\phi_n(\omega) = \begin{cases} 1; \ |\omega| \le (1-\gamma)\omega_n; \\ \cos\left[\frac{\pi}{2}\beta\left(\frac{1}{2\gamma\omega_n}(|\omega| - (1-\gamma)\omega_n)\right)\right]; \\ (1-\gamma)\omega_n \le |\omega| \le (1+\gamma)\omega_n; \\ 0; \ \textit{other}; \end{cases} \tag{1}$$

$$\psi_n(\omega) = \begin{cases} 1; (1+\gamma)\omega_n \le |\omega| \le (1-\gamma)\omega_{n+1}; \\ \cos\left[\frac{\pi}{2}\beta\left(\frac{1}{2\gamma\omega_{n+1}}(|\omega| - (1-\gamma)\omega_{n+1})\right)\right]; \\ (1-\gamma)\omega_{n+1} \le |\omega| \le (1+\gamma)\omega_n; \\ \sin\left[\frac{\pi}{2}\beta\left(\frac{1}{2\gamma\omega_n}(|\omega| - (1-\gamma)\omega_{n+1})\right)\right]; \\ (1-\gamma)\omega_n \le |\omega| \le (1+\gamma)\omega_n; \\ 0; \qquad \text{other}; \end{cases} \tag{2}$$

where the transition function $\beta(\omega)$ and the coefficient γ with respect to partial parameter are respectively

$$\beta(\omega) = \omega^4\left(35 - 84\omega + 70\omega^2 - 20\omega^3\right), \tag{3}$$

$$\gamma < \min\left(\frac{\omega_{n+1}-\omega_n}{\omega_{n+1}+\omega_n}\right), \tau_n = \gamma\omega_n, 0 < \gamma < 1 \ . \tag{4}$$

Step4: The inner product of the original signal and the empirical wavelet function and scale function respectively is defined as the detail correlation coefficient $W_f^{\varepsilon}(n,t)$ and the approximate correlation coefficient $W_f^{\varepsilon}(0,t)$ and the Fourier to transform and the inverse transform are set to $F(\cdot)$ and $F^{-1}(\cdot)$

$$\begin{aligned} W_f^{\varepsilon}(n,t) &= \langle f(t), \psi_n(t)\rangle = \int^f(\tau)\overline{\psi_n(\tau - t)}d\tau \\ &= F^{-1}\left(\hat{f}(\omega)\hat{\psi}_n(\omega)\right) \end{aligned} \tag{5}$$

$$\begin{aligned} W_f^{\varepsilon}(0,t) &= \langle f(t), \phi_1(t)\rangle = \int^f(\tau)\overline{\phi_1(\tau - t)}d\tau \\ &= F^{-1}\left(\hat{f}(\omega)\hat{\phi}_1(\omega)\right). \end{aligned} \tag{6}$$

In the above equation: $\psi_n(t)$ is the empirical wavelet function; $\phi_1(t)$ is the empirical scale function; $\overline{\psi_n(\tau - t)}$ is the complex conjugate of $\psi_n(t)$. Where $\hat{f}(\omega)$,$\hat{\phi}_1(\omega)$ and $\hat{\psi}_n(\omega)$ represent the Fourier transforms of $f(t)$, $\phi_1(t)$ and $\psi_n(t)$ respectively. Then the signal can be reconstructed as:

$$\begin{aligned} f(t) &= W_f^{\varepsilon}(0,t) * \emptyset_1(t) + \sum_{n=1}^{N} W_f^{\varepsilon}(n,t) * \psi_n(t) \\ &= F^{-1}\left(\hat{W}_f^{\varepsilon}(0,\omega)\hat{\emptyset}_1(\omega) + \sum_{n=1}^{N}\hat{W}_f^{\varepsilon}(n,\omega)\hat{\psi}_n(\omega)\right) \end{aligned} \tag{7}$$

where $\hat{W}_f^{\varepsilon}(0,\omega)$ and $\hat{W}_f^{\varepsilon}(n,\omega)$ represent the Fourier transforms of $\hat{W}_f^{\varepsilon}(0,t)$ and $\hat{W}_f^{\varepsilon}(n,t)$ respectively. Finally, the empirical wavelet function of the original signal is defined as follows

$$\begin{cases} f_0(t) = W_f^{\varepsilon}(0,t) * \phi_1(t) \\ f_k(t) = W_f^{\varepsilon}(k,t) * \psi_k(t) \end{cases} \tag{8}$$

2.2. Correlation kurtosis

When the inner ring or outer ring of a bearing fails, a signal usually exhibits the characteristics of cyclic stability, which encompasses the common properties of pulse and periodic signals. Therefore, when detecting bearing faults, it is necessary to identify automatically the cyclic stationary information of components. The correlation kurtosis based on the squared envelope of the demodulated signal is sensitive to the periodic impact characteristics of related bearing faults [24].

For signal f(t), the signal in the nth frequency band Λ_n is $f_n(t)$, $n = 1,2,\ldots,N$. The squared envelope in Λ_n is $|f_n(t)|^2$, and the squared envelope is autocorrelated:

$$\hat{R}_{ff}(\tau) = \frac{1}{L-q}\sum_{\mathrm{i}=1}^{L-q} |f_n(t_i)|^2 \cdot |f_n(t_i+\tau)|^2 \tag{9}$$

where $\tau = q/f_s$ represents the delay factor, $q = 0,1,\ldots L-1$, f_s is the sampling frequency, and L is the length of the signal.

The correlation kurtosis in the frequency band Λ_n is defined as:

$$\mathrm{CK}_n = \frac{\sum_{\mathrm{i}=1}^{\mathrm{L}/2}\left[\hat{R}_{ff}(\mathrm{i}) - \min\left(\hat{R}_{ff}(\tau)\right)\right]^4}{\left[\sum_{\mathrm{i}=1}^{\mathrm{L}/2}\left[\hat{R}_{ff}(\mathrm{i}) - \min\left(\hat{R}_{ff}(\tau)\right)\right]^2\right]^2} \ . \tag{10}$$

3. Improvement of EWT

Different components in a signal will generally be found in different frequency bands in the frequency spectrum, and information related to bearing failure will be concentrated near the center frequency. When separating strong noise and non-stationary signals, the traditional EWT may separate too many invalid components or break the same component into several sections, making it difficult to locate the fault information [25]. The EEWT is to use order statistics filter, which can calculate the upper envelope based on the characteristics of spectrum fluctuations. In this paper, the minimum value of the envelope is used as a boundary to construct a filter bank. The bearing fault simulation test presented in this research demonstrates that the method of dividing boundaries by the characteristics of spectral fluctuations and energy distribution is simpler and faster than using scale-space representation. The flowchart of the enhanced EWT for rolling bearing fault diagnosis is shown in figure 1.

In the enhanced empirical wavelet transform, the most important is the order statistics filter, which has three modes: maximum filter, median filter, and minimum filter. This paper uses the maximum filter to calculate the envelope of $f(t)$. When the length of signal $f(t)$ is L,$i \in [1,L]$, its basic steps are as follows.

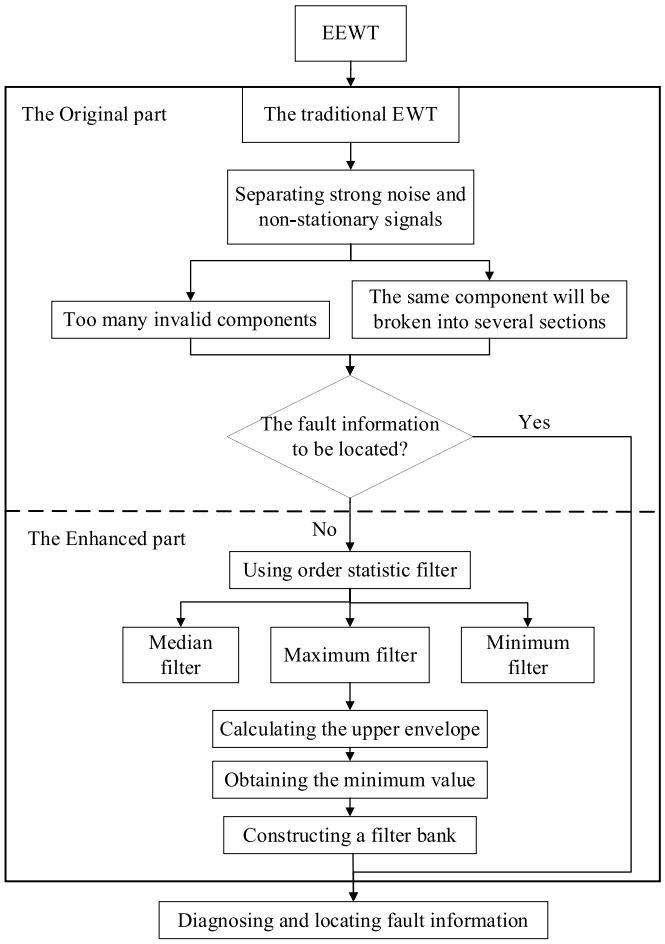

Figure 1. Flowchart of the enhanced empirical wavelet transform for rolling bearing fault diagnosis.

Step1: The sliding window will divide the signal into $L - W_{\mathrm{OSF}} + 1$ groups and the window width W_{OSF} is an odd number with a minimum of 3.

Step2: The data in the window will be extracted. The maximum value in $[f_1(t), f_2(t) \ldots, f_{W_{\mathrm{OSF}}}(t)]$ will be extracted and stored in $E_u(1)$.

Step3: The window will be moved in steps of 1. The maximum value in $[f_2(t), f_3(t) \ldots, f_{W_{\mathrm{OSF}}+1}(t)]$ will be extracted and stored in $E_u(2)$.

Step4: After the above steps are repeated, the new array can be obtained

$$E_u = \sum_{j=1}^{L-W_{\mathrm{OSF}}+1} \max\left\{F_j(\mathrm{t}), F_{j+1}(\mathrm{t}) \ldots, F_{j+W_{\mathrm{OSF}}-1}(\mathrm{t})\right\} . \tag{11}$$

Since the new array approximates the upper envelope of the spectrum, the minimum point of the envelope will be considered as the dividing point between different components. After normalizing the minimum point to $[0, \pi]$, it will be used to construct a filter bank.

4. Simulation verification

There is a non-stationary periodic shock signal with Gaussian white noise defined by taking the simulated signal as an example:

$$\begin{cases} s_{c1} = 5\cos(2\pi \cdot f_1 t) \times \sin(2\pi \cdot f_2 t + \sin(2\pi \cdot f_3 t)) \\ s_{c2} = \sum_{i=1}^{M} 6e^{-g\times 2\pi f_n^i t} \times \sin\left(2\pi f_n^i t \times \sqrt{1-g^2}\right) \\ s_1 = s_{c1} + s_{c2} + \zeta \end{cases} \tag{12}$$

The simulation signal s_1 contains three components: the first component s_{c1} is the modulation signal with the center frequency of 1000 Hz, where $f_1 = 50$ Hz, $f_2 = 1000$ Hz, $f_3 = 100$ Hz. The second component s_{c2} is the periodic shock signal of fault information with the center frequency of 3000 Hz, its natural frequency is $f_n = 1600$ Hz, the damping coefficient $g = 0.02$ and the period of the shock is $T = 0.03$ s. The third component ζ is noise with a Signal Noise Ratio of -2 dB. The waveform, frequency spectrum and envelope spectrum of the simulated signal are shown in figure 2.

It can be found from figure 2 that the periodic impact of the signal waveform (figure 2(a)) is not obvious and it is impossible to judge whether the impact is periodic. It can be seen from the frequency spectrum (figure 2(b)) that the signal contains a lot of noise, the fault information is concentrated around 3000 Hz and the amplitude is very low. The characteristic frequency of the fault and its harmonics cannot be found in the envelope spectrum (figure 2(c)). As shown in figure 3, the upper envelope of the frequency spectrum can be calculated through the order statistical filter. The wave characteristic of the envelope is like the wave character of the frequency spectrum and the part with the center frequency of 1000 Hz and the part with 3000 Hz are included.

If the minimum value of the upper envelope is used as the boundary and substituted into the EWT for segmentation and filtering, the spectrum will be divided into eight parts. The modulation component is the second component and the fault component is the fifth component. The correlation kurtosis of each component is calculated as shown in figure 4.

According to the correlation kurtosis, it can be predicted that the fifth component may contain the most fault information. Extracting this component and displaying its waveform (figure 5(a)) and envelope spectrum (figure 5(b)) are as shown in figure 5.

There is impulse information in the waveform of this component and these shocks are periodic. Compared with the original signal, the noise is suppressed and the component with a center frequency of 1000 Hz is separated. There are characteristic frequencies and their harmonics in the envelope spectrum of this component and it can be considered that the fault information has been successfully extracted.

Using the original EWT to process the signal, it can be found from figure 6 that the signal is divided into 14 parts, where the third part is modulation information. A boundary

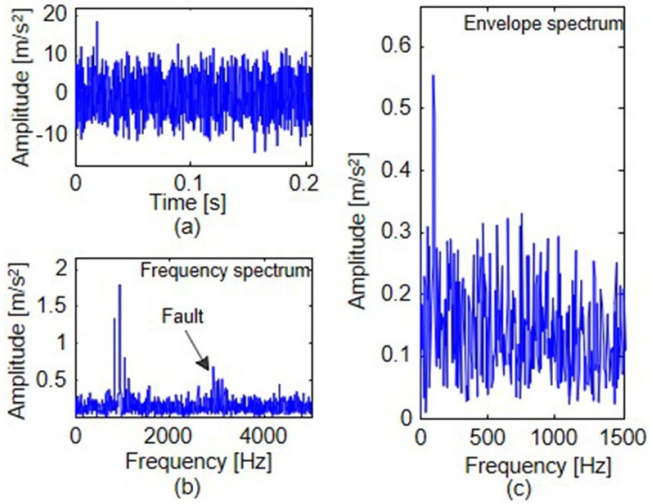

Figure 2. The waveform (a), its spectrum (b), and its envelope spectrum (c).

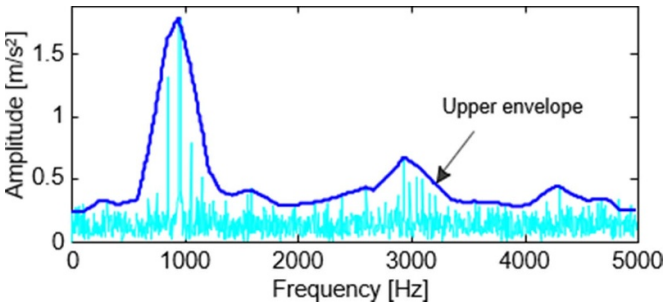

Figure 3. Calculating the upper envelope by order statistics filter.

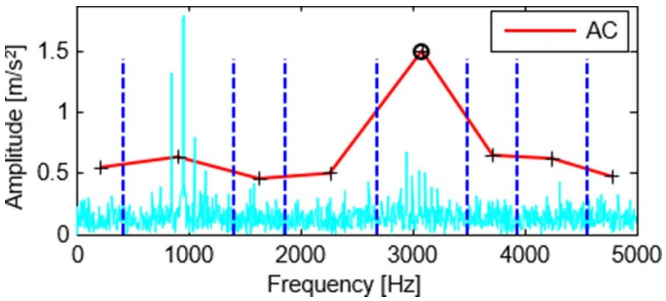

Figure 4. Boundaries and CK of each component.

appears at 3000 Hz and the fault information is divided into two parts which brings trouble to the identification of the fault information.

After calculating the kurtosis of each component, the relationship between the kurtosis and the frequency band is shown in figure 7. It can be found that the kurtosis of the fault information separated into two parts is not the largest, while the part with the largest kurtosis is in the frequency band with higher frequency and the frequency band is very narrow. In addition, single pulse or random pulse is easy to appear in narrow band and this information exerts a great impact on the kurtosis.

As shown in figure 8, the component is extracted and its waveform is displayed. This component is a component of

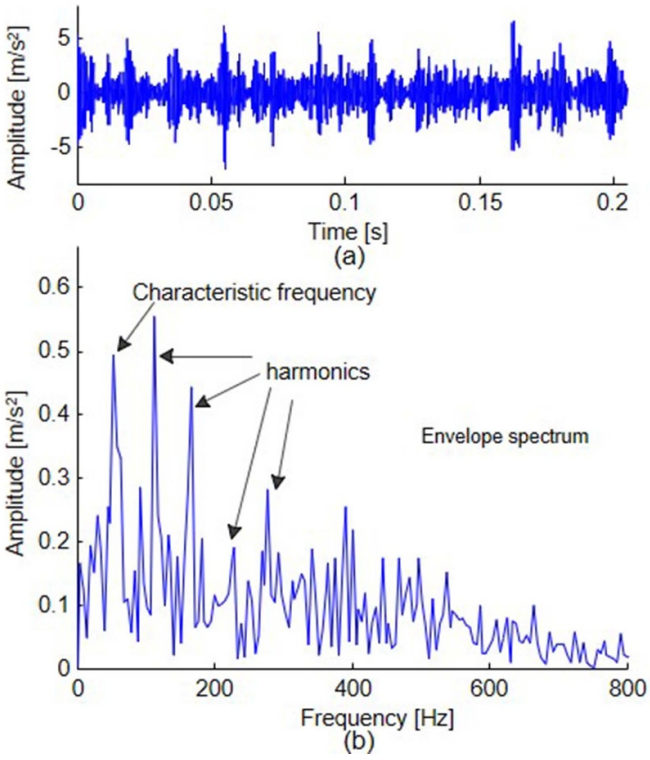

Figure 5. The component with maximum CK (a) and its envelope spectrum (b).

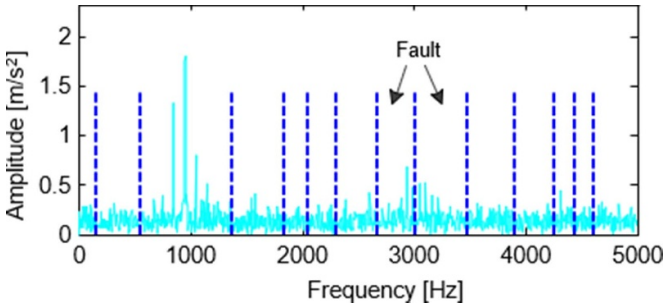

Figure 6. Boundaries decomposed by EWT.

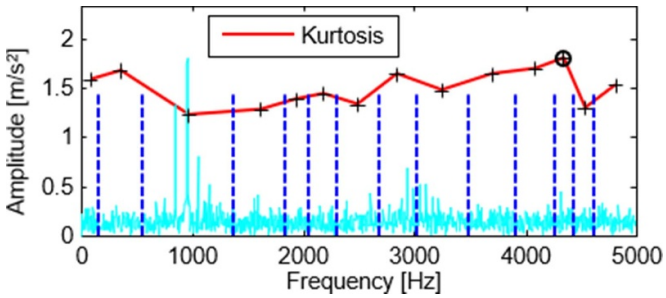

Figure 7. Boundaries and CK of each component.

high-frequency and low-frequency phase modulation and it is impossible to determine whether it contains periodic impact information.

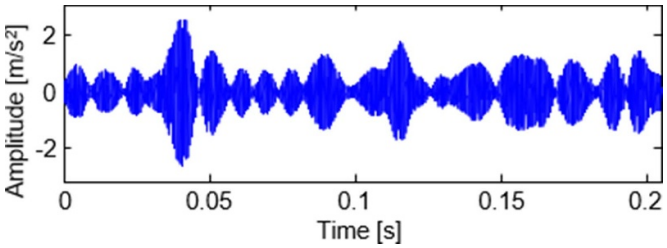

Figure 8. The component with maximum kurtosis.

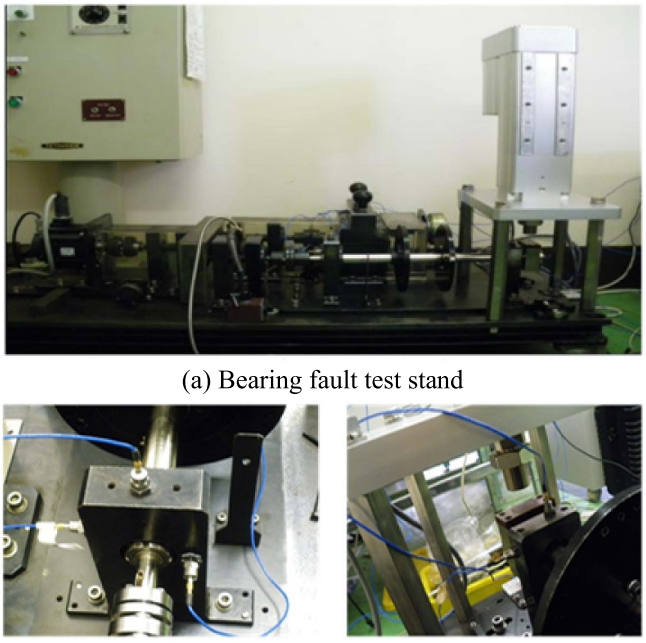

(a) Bearing fault test stand

(b) Sensors

Figure 9. Bearing fault test stand (a) and the installation locations of sensors (b).

5. Engineering application

Figure 9 shows the bearing fault test stand of Japan's National Mie University, on which the bearing failure simulation experiment was carried out.

The bearing model selected in this experiment is NU204 with outer ring damage width of 0.3 mm and depth of 0.05 mm. Figure 10 shows the location of outer ring damage (figure 10(a)) and the size of outer ring (figure 10(b)). There exists that the static load is 150 kg, the shaft speed is 1500 rpm s^{-1}, the characteristic frequency of the outer ring is $f_O = 100$Hz, and the period is $T_O = 0.01$ s.

Figure 11 shows the collected one of signals (figure 11(a)) and its spectrum (figure 11(b)). The large amount of noise contained in the waveform masks the impact information in the signal and the waveform in the frequency spectrum is also masked by strong noise.

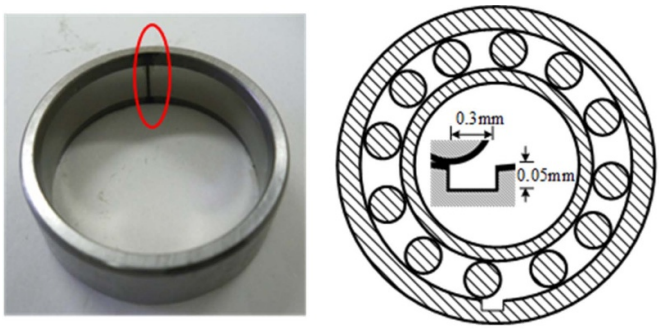

(a) Location (b)Size of outer ring

Figure 10. Location of outer ring damage (a) and size of outer ring (b).

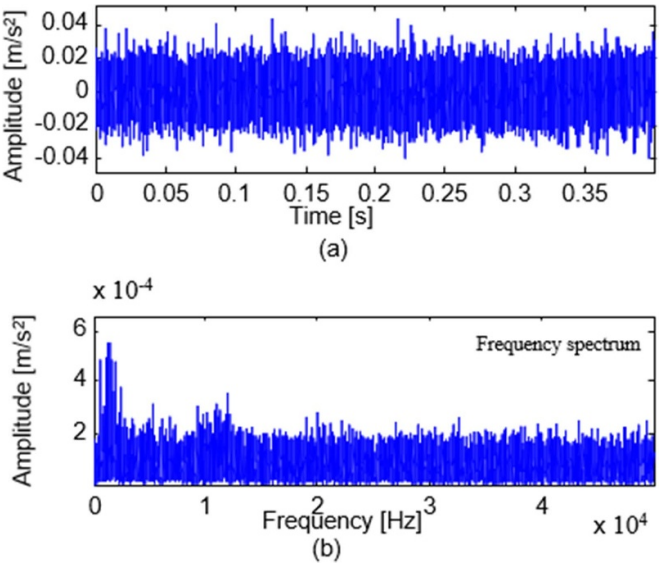

Figure 11. Bearing outer ring fault signal (a) and its spectrum (b).

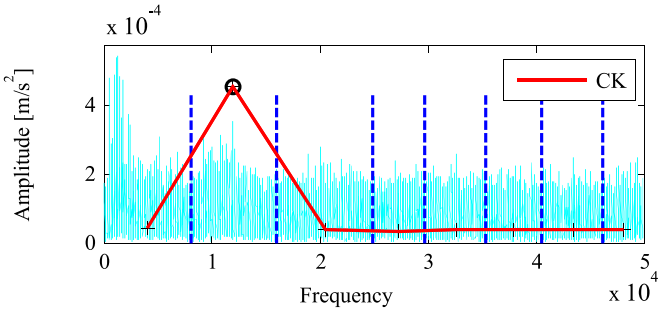

Figure 12. Boundaries and CK of each component.

The method proposed in this article is used to process the mentioned signal. It can be seen from figure 12 that the signal is divided into 8 parts. Although the amplitude of the frequency spectrum of the first component is higher, the correlation kurtosis value of the second part is the highest, so the fault information of the bearing outer ring could be concentrated in the part with a center frequency of 11 000 Hz.

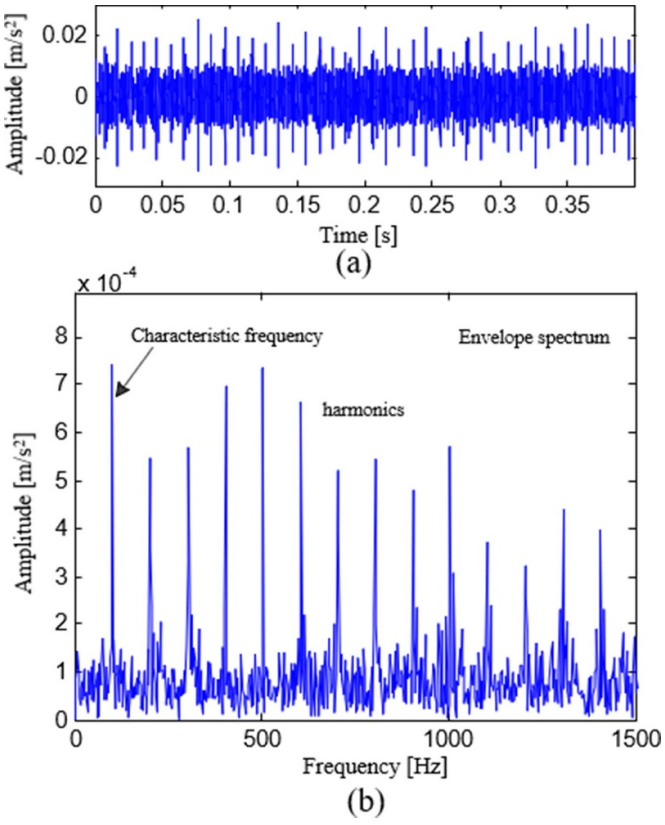

Figure 13. The component with maximum CK (a) and its envelope spectrum (b).

From figure 13, extracting the component with the largest correlation kurtosis (figure 13(a)) and calculating its envelope spectrum (figure 13(b)) reveals that although this component contains noise, it also contains very distinct periodic shocks. Through calculation, it can be known that this period coincides with the fault period of the bearing outer ring. From the envelope spectrum (b) of the figure 13, we can also find the fault characteristic frequency and its multiple frequency of the bearing outer ring. Therefore, the outer ring of the bearing is damaged. The method proposed in this paper can be effectively applied to the fault diagnosis of bearing outer ring.

6. Conclusion

In this paper, with respect to the problem that the conventional wavelet transform does not work well when dealing with strong noise and non-smooth signals, which may lead to modal mixing or even decomposition of too many invalid components. A rolling bearing fault diagnosis method combining EEWT and CK is proposed to effectively extract fault information from strong noise signals. The proposed method provides an effective scheme that can be used for successful practical applications in rolling bearing fault diagnosis and gives directions for future signal research and analysis for bearing fault diagnosis.

The results of the simulated and experimental signals show that, compared with the conventional EWT method, The proposed method not only obtains fewer components and the largest number of frequency bands when filtering the fault information by extracting the component with the largest CK, but also successfully extracts the obvious periodic shock information present in the component, and the period of this periodic shock information is consistent with the period of the bearing outer ring fault. At the same time, this method which employs an effective combination of EWT and CK can not only make full use of their respective advantages, but also extract the characteristic frequency and its frequency doubling of bearing outer ring fault, making it applicable to the field of bearing failure or other mechanical fault diagnosis directions.

Data availability statement

The data generated and/or analysed during the current study are not publicly available for legal/ethical reasons but are available from the corresponding author on reasonable request.

Acknowledgments

The authors would like to gratefully acknowledge Professor Yonggang Xu for providing the experimental data of the bearing fault simulator. The authors offer sincere gratitude to the Key Laboratory of Advanced Manufacturing Technology for its support. Finally, the authors would like to thank the editors and reviewers for their valuable comments and constructive suggestions

ORCID iDs

Jijun Xue https://orcid.org/0000-0002-1701-579X
Hao Xu https://orcid.org/0000-0003-3474-0210
Xiaodong Liu https://orcid.org/0000-0002-2702-4972
Di Zhang https://orcid.org/0000-0002-7967-1661
Yonggang Xu https://orcid.org/0000-0002-2206-8968

References

[1] Xu Y, Zhang K and Ma C 2019 Adaptive kurtogram and its applications in rolling bearing fault diagnosis *Signal Process.* **130** 87–107
[2] Li S *et al* 2019 A review on the signal processing methods of rotating machinery fault diagnosis *2019 IEEE 8th Joint Int. Information Technology and Artificial Intelligence Conf. (ITAIC)* (IEEE)
[3] Huang N, Shen Z and Long S 1998 The empirical mode decomposition and the Hilbert spectrum for nonlinear and nonstationary time series analysis *Proc. Math. Phys. Eng. Sci.* **454** 903–95
[4] Feng Z and Chu F 2013 Frequency demodulation analysis method for fault diagnosis of planetary gearboxes *Proc. CSEE* **33** 112–7
[5] Lei Y, Zuo M and He Z 2010 A multidimensional hybrid intelligent method for gear fault diagnosis *Expert Syst. Appl.* **37** 1419–30
[6] Georgoulas G *et al* 2013 Bearing fault detection based on hybrid ensemble detector and empirical mode decomposition *Mech. Syst. Signal Process.* **41** 510–25

[7] Rehman N U and Mandic D P 2010 Multivariate empirical mode decomposition *Proc. R. Soc.* A **466** 1291–302
[8] Rehman N U and Mandic D P 2011 Filter bank property of multivariate empirical mode decomposition *IEEE Trans. Signal Process.* **59** 2421–6
[9] Rehman N U, Park C, Huang N and Mandic D P 2013 EMD via MEMD: multivariate noise-aided computation of standard emd *Adv. Adapt. Data Anal.* **05** 1350007
[10] Li Y, Xu M, Zhao H, Wei Y and Huang W 2015 A new rotating machinery fault diagnosis method based on improved local mean decomposition *Digit. Signal Process.* **46** 201–14
[11] Chen G and Wang Z 2012 A signal decomposition theorem with Hilbert transform and its application to narrowband time series with closely spaced frequency components *Mech. Syst. Signal Process.* **28** 258–79
[12] Wang Z, Xin Y, Xing J and Ren W-X 2017 Hilbert low-pass filter of non-stationary time sequence using analytical mode decomposition *J. Vib. Control* **23** 2444–69
[13] Zhang K, Xu Y and Chen P 2020 Feature extraction by enhanced analytical mode decomposition based on order statistics filter *Measurement* **173** 108620
[14] Wei D, Jiang H, Shao H, Li X and Lin Y 2019 An optimal variational mode decomposition for rolling bearing fault feature extraction *Meas. Sci. Technol.* **30** 055004
[15] Gilles J 2013 Empirical wavelet transform *IEEE Trans. Signal Process.* **61** 3999–4010
[16] Cao H, Fan F, Zhou K and He Z 2016 Wheel-bearing fault diagnosis of trains using empirical wavelet transform *Measurement* **82** 439–49
[17] Zhu W and Feng Z 2016 Fault diagnosis of planetary gearbox based on improved empirical wavelet transform *Chin. J. Sci. Instrum.* **37** 2193–201
[18] Duan C and Zhang R 2019 Locomotive bearing fault diagnosis using an improved empirical wavelet transform *China Mech. Eng.* **30** 631–7
[19] Chen J, Pan J, Li Z, Zi Y and Chen X 2016 Generator bearing fault diagnosis for wind turbine via empirical wavelet transform using measured vibration signals *Renew. Energy* **89** 80–92
[20] Jiang Y, Zhu H and Li Z 2016 A new compound faults detection method for rolling bearings based on empirical wavelet transform and chaotic oscillator *Chaos Solitons Fractals* **89** 8–19
[21] Yao R, Jiang H, Wu Z and Wang K 2021 Periodicity-enhanced sparse representation for rolling bearing incipient fault detection *ISA Trans.* **118** 219–37
[22] Yao R, Jiang H, Li X and Cao J 2022 Bearing incipient fault feature extraction using adaptive period matching enhanced sparse representation *Mech. Syst. Signal Process.* **166** 108467
[23] He Y, Wang H, Xue H and Zhang T 2021 Research on unknown fault diagnosis of rolling bearings based on parameter-adaptive maximum correlation kurtosis deconvolution *Rev. Sci. Instrum.* **92** 055103
[24] Gao Z, Lin J, Wang X and Xu X 2017 Bearing fault detection based on empirical wavelet transform and correlated kurtosis by acoustic emission *Materials* **10** 571
[25] Hu Y, Tu X, Li F, Li H and Meng G 2017 An adaptive and tacholess order analysis method based on enhanced empirical wavelet transform for fault detection of bearings with varying speeds *J. Sound Vib.* **409** 241–55